Available online at www.sciencedirect.com
ScienceDirect
ELSEVIER
Ceramics International 35 (2009) 3235–3239
CERAMICS INTERNATIONAL
www.elsevier.com/locate/ceramint

Crystallization behavior of $Bi_{1.25}Y_{1.75}Fe_5O_{12}$ prepared by coprecipitation process

Yen-Pei Fu *, Kar-Kit Lew

Department of Materials Science and Engineering, National Dong Hwa University, Shou-Feng, Hualien 974, Taiwan

Received 13 February 2009; received in revised form 21 April 2009; accepted 19 May 2009
Available online 7 July 2009

Abstract

A non-isothermal study of the crystallization kinetic of coprecipitation of $Bi_{1.25}Y_{1.75}Fe_5O_{12}$ was carried out by differential scanning calorimetry (DSC). The Avrami exponent n suggesting the dimensionality of crystal growth was determined using the Ozawa equation. From non-isothermal DSC data presented values in range of 775–1023 kJ/mol and 3.28–2.10 for the activation energy of crystallization and the Avrami exponent, respectively. These Avrami exponent values were consistent with surface and internal crystallizations growth simultaneously.

Keywords: A. Powder: chemical preparation; C. Thermal properties; E. Soft magnets

1. Introduction

Yttrium iron garnet (YIG) was extensively studied owing to its interesting physical properties. For example, this material possesses the highest quality factor in microwave regime, and the smallest linewidth in magnetic resonance among magnetic materials [1,2]. YIG-based materials are important components of electronics products, such as circulators, oscillators, and phase shifter. However, YIG is hardly used in multilayer microwave components because of its high sintering temperature (>1350 °C). The sintering temperature of YIG is generally higher than the melting point of highly conductive metals such as Ag–Pd alloy (1145 °C) [3]. Previous investigation have shown that Bi-substituted and 2Ca–V-substituted YIG powders can be prepared at much lower temperatures (<1100 °C) than that for preparing pure YIG due to their lower melting temperature, and the sintering temperature of these materials is much lower than YIG polycrystalline ceramics [4–6]. The basic property to evaluate magnetic ceramic for microwave application is the low power loss. Accordingly, low dielectric losses are required to increase the skin depth so as to ensure microwave to penetrate a large volume of magnetic ceramic. Loss tangent of the order of $<10^{-3}$ is desirable for microwave devices such as phase shifter, isolator, and circulator.

Magnetic fine particles are very attractive for magnetic ceramic research. This is because they have a single magnetic domain. Polycrystalline YIG and substituted YIG have attracted much attention for microwave device and magneto-optical applications [7]. The conventional method of producing these materials is by the solid-state reaction with oxide/carbonate and then calcining at a high temperature (≥ 1200 °C). The solid-state reaction method has some inherent disadvantages as follows: (1) chemical inhomogeneity, (2) coarser particle size, and (3) introduction of impurities during ball milling. In order to improve the performance and quality of Bi-YIG magnetic ceramics, coprecipitation is an alternative method of overcoming the deficiencies in the conventional solid-state reaction. In general, YIG-based powder can be prepared by using several chemical approaches such as sol–gel [8–11], sol–gel auto combustion method [12,13], spray pyrolysis process [14], and citrate method [15]. There have been many investigations on the microwave and magneto-optical properties, focused on correlations between the microstructure, composition, and magnetic properties of Bi-substituted YIG. However, there seem to be almost no reports on the crystallization characterization for these materials. Therefore, coprecipitation was used in this study to produce $Bi_{1.25}Y_{1.75}Fe_5O_{12}$ powder and studied its non-isothermal crystallization kinetics.

---

* Corresponding author. Tel.: +886 3 863 4209; fax: +886 3 863 4200.
E-mail address: d887503@alumni.nthu.edu.tw (Y.-P. Fu).

0272-8842/$36.00 © 2009 Elsevier Ltd and Techna Group S.r.l. All rights reserved.
doi:10.1016/j.ceramint.2009.05.038

2. Experimental procedures

2.1. Preparation of Bi-YIG powders

According to the stoichiometric composition of $Bi_{1.25}Y_{1.75}Fe_5O_{12}$, specified amounts of bismuth nitrate pentahydrate [$Bi(NO_3)_3\cdot 5H_2O$], yttrium nitrate hexahydrate [$Y(NO_3)_3\cdot 6H_2O$], and iron nitrate nonahydrate [$Fe(NO_3)_3\cdot 9H_2O$] were dissolved in a certain quantity of water. 28% ammonia solution (NH_4OH) was added rapidly into the stirred solution at room temperature. In the pH range of more than 8.7, the ratio of the cations in the powders was the same as that in the nitrate solution. The pH of the solution was controlled to be above 12. The obtained slurry was washed with alcohol to remove the alkaline ions and obtain a weak agglomeration of Bi-YIG powders, filtered and dried at 90 °C for 24 h. Then, the coprecipitate of the as-prepared $Bi_{1.25}Y_{1.75}Fe_5O_{12}$ powder was annealed at 700 °C for 2 h. This powder was mixed with a 3% poly(vinylalcohol) (PVA) binder and pressed into disk, which were sintered at 900 °C for 2 h in air. A disk was cut into a thin slab for microwave measurement.

2.2. Characterization

A computer-interfaced X-ray powder diffractometer (XRD) with Cu K_α radiation ($\lambda = 1.5418$ Å) (Model Rigaku D/Max-II, Tokyo, Japan) was used to identify the crystalline phase during crystallization process. BET surface area measurements were made by nitrogen adsorption employing a Micromeritics ASAP 2020 instrument (Norcross, GA, USA) and calculated using the five point Brunauer–Emmit–Teller (BET) theory. Mean particle size (D_{BET}) was calculated from the BET data according to the following equation assuming that the particles are closed sphere with smooth surface and uniform size: $D_{BET} = 6 \times 10^3/(\rho\text{th } S_{BET})$, where D_{BET} (nm) is the average particle size, S_{BET} is the measured specific surface area expressed in m^2/g and ρth is the theoretical density of the compound (g/cm^3). Differential scanning calorimetry (DSC; Model TG-DTA/DSC Setaram, Caluiro, France) was used to carry out the crystallization characterization of as-prepared Bi-YIG powders. A heating rate of 10–25 °C/min was used in DSC up to 900 °C in air. Thermal analysis was carried out under flowing air at 100 ml/min. A constant sample weight of 12.0 ± 0.2 mg was used for all measurements.

3. Results and discussion

Crystallization characterization of the Bi-YIG powder was estimated by non-isothermal DSC analysis. Fig. 1 shows the DSC curves of a sample at different heating rates ranging from 10 to 25 °C. With increasing heating rate, the exothermic peak shifts to a higher temperature. The XRD patterns of heat-treated samples at different temperatures 550–650 °C for 2 h are presented in Fig. 2. The Bi-YIG specimen was primary amorphous due to the broad low-intensity peak appeared at 32° diffraction angle. When the heat-treated temperature reached 575 °C, the specimen only revealed (4 2 0) very low-intensity peak. However, when the heat-treated temperature reached 600 °C, the specimen revealed (4 0 0), (4 2 0), and (4 2 2) peaks. With increasing heat-treated temperature, the broad hump associated with the amorphous phase decreased, and the intensity of XRD peaks increased as the amorphous phase got transformed into the crystalline phase, garnet. The volume fraction of crystallized phase increases with heat-treated temperatures. These results are consistent with DSC measurement results. The specific surface area and mean particle size of Bi-YIG powders heat treated at different temperatures are shown in Fig. 3. The result indicates that the particle size increased with annealing temperature. Compared XRD with BET results, we can conclude that when garnet crystalline phase appears, which heat-treated temperature is about 600 °C, the mean particle size requires larger than 75 nm prepared by coprecipitation process.

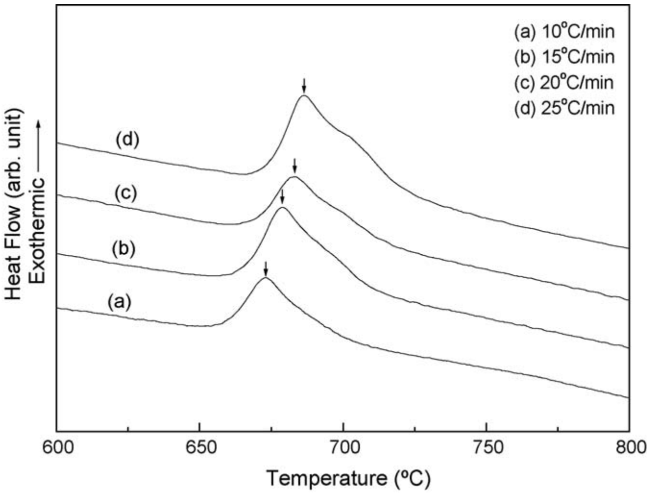

Fig. 1. Differential scanning calorimetry curves of as-precipitated $Bi_{1.25}Y_{1.75}Fe_5O_{12}$ powder at different heating rates of 10, 15, 20, and 25 °C/min.

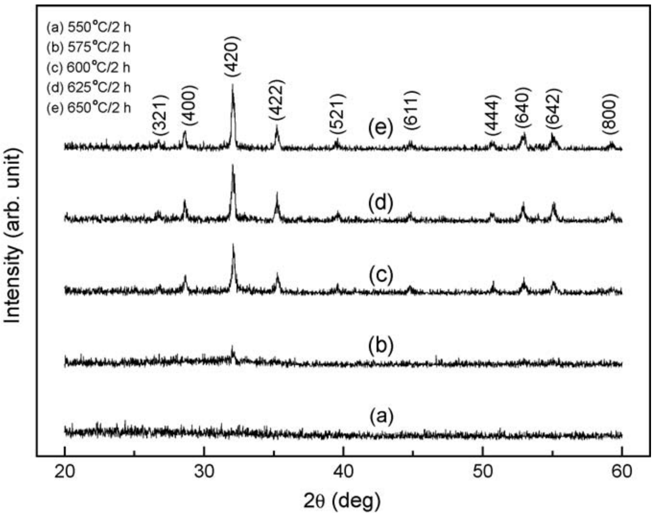

Fig. 2. X-ray diffraction results of as-precipitated $Bi_{1.25}Y_{1.75}Fe_5O_{12}$powders heat treated at various temperatures for 2 h.

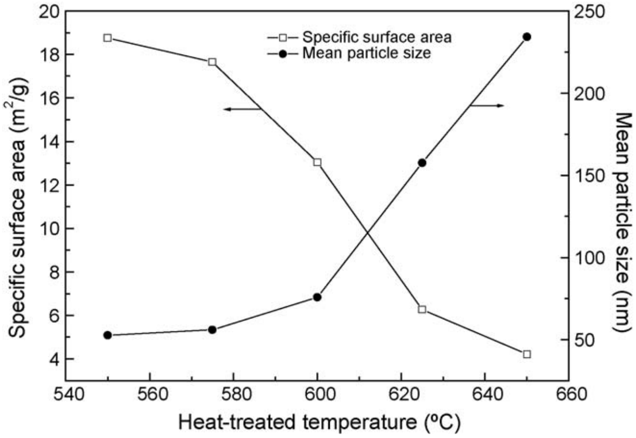

Fig. 3. Dependence of specific surface area and mean particle size on the heat-treated temperature for $Bi_{1.25}Y_{1.75}Fe_5O_{12}$ powder derived from coprecipitation process.

The activation of crystallization peaks depending on the DSC scan rates can be used to estimate the activation energy of crystallization by using following Kissinger analysis [16]. Through the change in the peak crystallization temperature (T_p) with respect to heating rate, the activation energy of crystallization could be determined using the equation:

$$\mathrm{Log}_e(T_\mathrm{p}^2/\Phi) = E/RT_\mathrm{p} + \mathrm{constant} \qquad (1)$$

where, E is the activation energy for crystallization. T_p is the temperature corresponding to the maximum of the DSC crystallization peak, R is the gas constant (8.314 J/mol), and Φ is the heating rate. The Φ used are 10, 15, 20, and 25 °C/min. If the plot of $\mathrm{Log}_e(T_\mathrm{p}{}^2/\Phi)$ versus $1/T_\mathrm{p}$ is a straight line, and the slope is E/R, and the activation energy of the crystallization could be estimated. Fig. 4 shows the Kissinger plot of the as-prepared $Bi_{1.25}Y_{1.75}Fe_5O_{12}$ powder. The activation energy of crystallization is determined using the Kissinger equation from the slope and is equal to 528.14 kJ/mol.

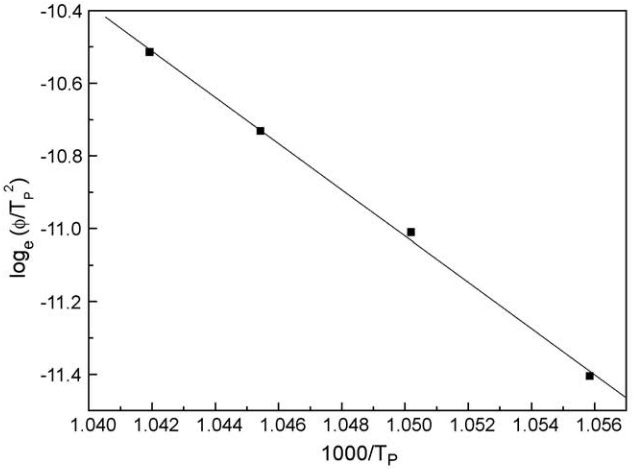

Fig. 4. Plot of $\mathrm{Log}_e(T_\mathrm{p}{}^2/\Phi)$ against $1000/T_\mathrm{p}$ for determining crystallization activation energy of $Bi_{1.25}Y_{1.75}Fe_5O_{12}$.

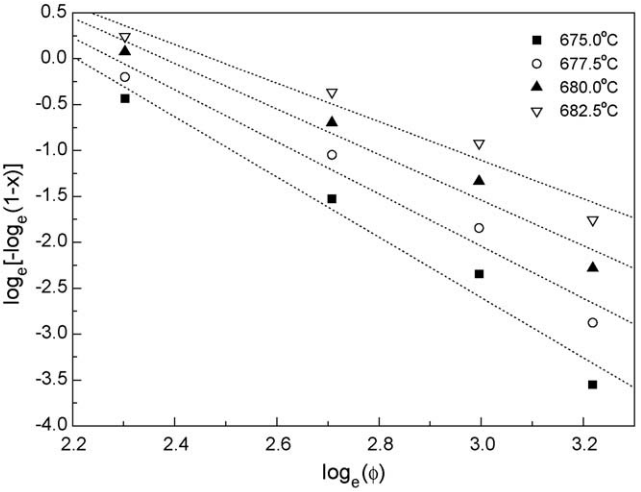

Fig. 5. Plot of $\mathrm{Log}_e[-\mathrm{Log}_e(1-X)]$ versus $\mathrm{Log}_e\Phi$ for determining Avrami constant n at different specific temperatures.

Moreover, the Avrami exponent n can be determined from DSC results. The value of the Avrami parameter n, which is a measure of the dimensionality of transformation, is determined using the Ozawa equation [17]:

$$d\{\mathrm{Log}_e[-\mathrm{Log}_e(1-X)]\}/d\mathrm{Log}_e\Phi = -n \qquad (2)$$

where, Φ is the different heating rates, X is the volume fraction crystallized at a specified temperature T, X is the given ratio of the partial area crystallized at a certain temperature to the total area of the crystallization exotherm. Here, the total area of the crystallization exotherm is between the temperature T_i at which crystallization just begins and the temperature T_f at which crystallization is complete. The partial area crystallized at a certain temperature is between T_i and T [18]. A plot of $\mathrm{Log}_e[-\mathrm{Log}_e(1-X)]$ versus $\mathrm{Log}_e\Phi$ should be a straight line from the slope, which n can be calculated. An n close to 3 indicates bulk or three-dimensional crystal growth and an n close to 1 indicates surface growth. Intermediate values of n between 1 and 3 indicate that surface and internal crystallizations occur simultaneously [19]. The Ozawa plot of $\mathrm{Log}_e[-\mathrm{Log}_e(1-X)]$ versus $\mathrm{Log}_e\Phi$ is shown in Fig. 5. Here, the volume fraction crystallized was calculated at different specific temperatures in the range of 675.0–682.5 °C. The values of n are determined form the slope of the plot were 3.28, 2.84, 2.48, and 2.10 for 675.0, 677.5, 680.0, and 682.5 °C, respectively. This indicates that the crystallization dominated by surface and internal crystallization growth simultaneously. Summary of crystallization parameters is listed in Table 1.

Table 1
Crystallization parameters of $Bi_{1.25}Y_{1.75}Fe_5O_{12}$ at different specific temperatures.

Temperature (°C)	Avrami constant (n)	E_a (kJ/mol)
675.0	3.28	775
677.5	2.84	831
680.0	2.48	899
682.5	2.10	1023

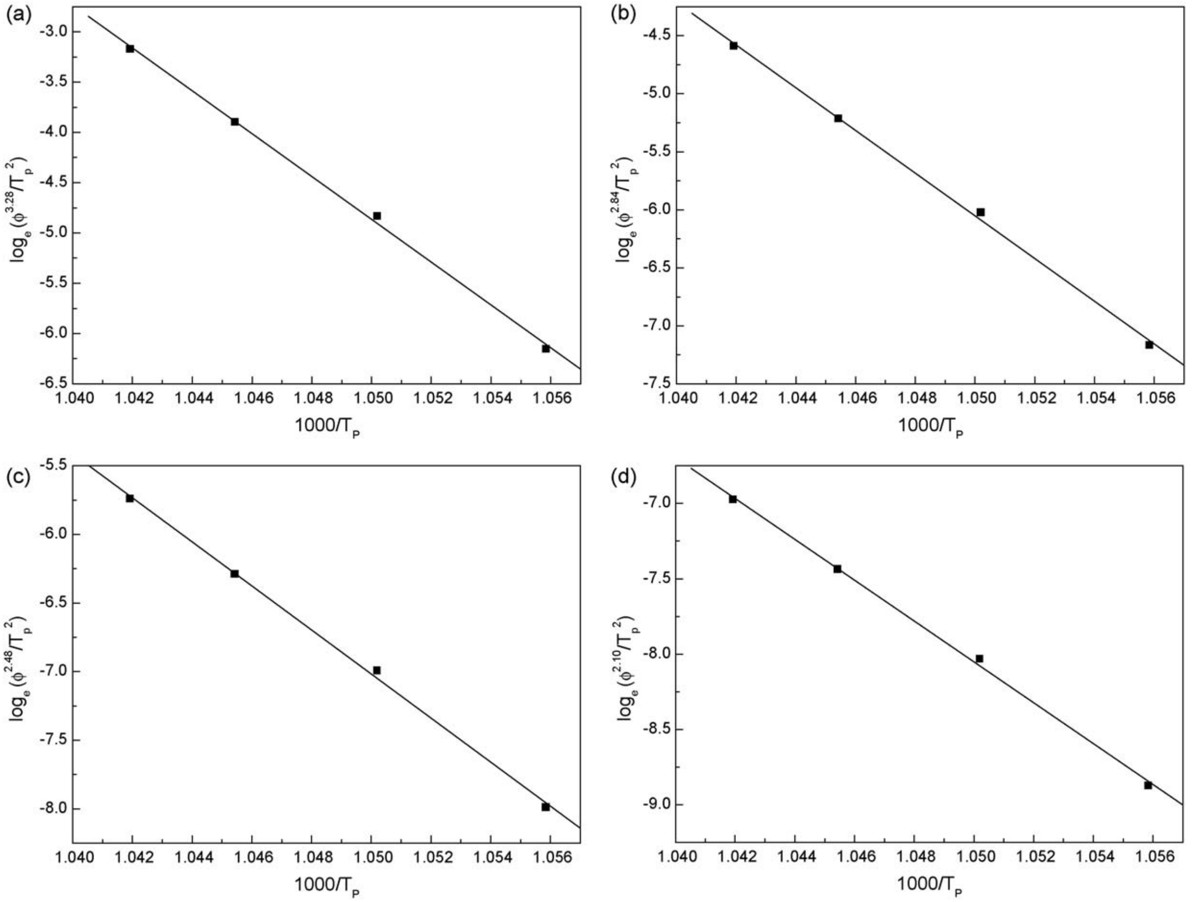

Fig. 6. Plot in accordance with Matusita and Sakka equation for determining activation energy for crystallization at different specific temperatures: (a) 675.0 °C; (b) 677.5 °C; (c) 680.0 °C; (d) 682.5 °C.

Matusita and Sakka [20,21] proposed that the Kissinger model is only valid when crystal growth occurs on a specified number of nuclei. They modified the Kissinger equation to account for nucleation and crystallization growth occurring simultaneously to

$$\mathrm{Log}_e(\Phi^n/T_\mathrm{p}^2) = -mE_\mathrm{c}/RT_\mathrm{p} + \text{constant} \tag{3}$$

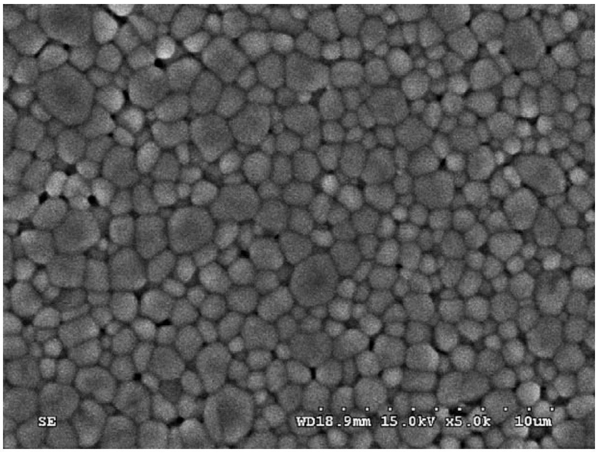

Fig. 7. Microstructure of $Bi_{1.25}Y_{1.75}Fe_5O_{12}$ specimen sintered at 900 °C for 2 h.

where, E_c is the activation energy of crystallization and m represents the dimensionality of the crystalline phase. n and m are corresponded to each other through the relation $m = n - 1$. Fig. 6(a–d) shows the Matusita and Sakka plot for the determined of activation energy of crystallization. It is found that the values of n are in the range of 3.28–2.10 and activation energy in the range of 775–1024 kJ/mol at different specific temperatures ranging from 675.0 to 682.5 °C. The detailed n and activation energy values are shown in Table 1.

The microstructure will significantly influence the magnetic properties for Bi-YIG materials. Fig. 7 illustrates the microstructure of $Bi_{1.25}Y_{1.75}Fe_5O_{12}$ specimen. The result reveals that the grain sizes are distribution in the range of 1–3 μm and high density. This indicates the coprecipitation powders have high sinterability compared with the conventional way of producing these materials by the solid-state reaction. According to the microstructure results, we also can speculate that $Bi_{1.25}Y_{1.75}Fe_5O_{12}$ specimen sintered from coprecipitation powder possesses higher magnetic properties compared with those one from solid-state reaction.

4. Conclusions

Non-isothermal crystallization kinetic of $Bi_{1.25}Y_{1.75}Fe_5O_{12}$ powder prepared by coprecipitation process has been investigated. The activation energy of crystallization was determined using the method proposed by Kissinger from the slope and is equal to 528.14 kJ/mol. The results revealed that the values of the *n* obtained experimentally are in the range of 3.28–2.10 for different specific temperature range of 675.0–682.5 °C. It was found that the controlling mechanism of crystallization is surface and internal crystallization growth simultaneously. By applying the modified Kissinger model, the activation energy of crystallization was found in the range of 775–1023 kJ/mol.

References

[1] Z. Yue, L. Li, J. Zhou, H. Zhang, Z. Ma, Z. Gui, Preparation and electromagnetic properties of ferrite-cordierite composites, Mater. Lett. 44 (2000) 279–283.

[2] H.M. Sung, C.J. Chen, W.S. Ko, H.C. Lin, Fine powder ferrite for multilayer chip inductors, IEEE Trans. Magn. 30 (1994) 4906–4908.

[3] H. Zhao, J. Zhou, Y. Bai, Z. Gui, L. Li, Effect of Bi-substitution on the dielectric properties of polycrystalline yttrium iron garnet, J. Magn. Magn. Mater. 280 (2004) 208–213.

[4] S. Geller, H.J. Williams, G.P. Espinosa, R.C. Sherwood, M.A. Gilleo, Reduction of the preparation temperature of polycrystalline garnets by bismuth substitution, Appl. Phys. Lett. 3 (1963) 21–22.

[5] K. Shinagawa, S. Taniguchi, Faraday effect of Bi-substituted rare-earth iron garnet, Jpn. J. Appl. Phys. 12 (1973) 465–1465.

[6] Y.Y. Song, S.C. Yu, W.T. Kim, J.R. Park, T.H. Kim, The effect of Bi_2O_3 addition on the microstructure and magnetic properties of YIG, J. Magn. Magn. Mater. 256 (1998) 177–181.

[7] N. Kawai, E. Komuro, T. Namikawa, Y. Yamazaki, Preparation of Bi-YIG particles for display devices, IEEE Trans. Magn. 30 (1994) 4446–4448.

[8] Z. Cheng, H. Yang, L. Yu, Y. Cui, S. Feng, Preparation and magnetic properties of $Y_3Fe_5O_{12}$ nanoparticles doped with the gadolinium oxide, J. Magn. Magn. Mater. 302 (2006) 259–262.

[9] V. Sankaranarayanan, N.S. Gajbhiye, Low-temperature preparation of ultrafine rare-earth iron garnets, J. Am. Ceram. Soc. 73 (1990) 1301–1307.

[10] C.S. Kuroda, T. Tanniyama, Y. Kitamoto, Y. Yamazaki, Magneto-optical properties and morphology of particulate film consisting of Bi-YIG coprecipitated particles, J. Magn. Magn. Mater. 241 (2002) 201–206.

[11] E. Garskaite, K. Gibson, A. Leleckaite, J. Glaser, D. Niznasky, A. Kareiva, H.J. Meter, On the synthesis and characterization of iron-containing garnet ($Y_3Fe_5O_{12}$, YIG and $Fe_3Al_5O_{12}$, IAG), Chem. Phys. 323 (2006) 204–210.

[12] S.H. Vajargah, H.R.M. Hosseini, Z.A. Nemati, Preparation and characterization of yttrium iron garnet (YIG) nanocrystalline powders by auto-combustion of nitrate-citrate gel, J. Alloys Compd. 430 (2007) 339–343.

[13] S.H. Vajargah, H.R.M. Hosseini, Z.A. Nemati, Synthesis of nanocrystalline yttrium iron garnet by sol–gel combustion process: the influence of pH of precursor solution, Mater. Sci. Eng. B 129 (2006) 211–215.

[14] D.S. Todorovsky, R.V. Todorovska, St. Groudeva-Zotova, Thermal decomposition of yttrium-iron citrates preparation in ethylene glycol medium, Mater. Lett. 55 (2002) 41–45.

[15] K. Matsumoto, K. Yamaguchi, T. Fujii, A. Ueno, Preparation of bismuth-substituted yttrium iron garnet powders by the citrate gel process, J. Appl. Phys. 69 (1991) 5918–5920.

[16] H.E. Kissinger, Variation of peak temperature with heating rate in different thermal analysis, J. Res. Natl. Bur. Stand. (U.S.) 57 (1956) 217–221.

[17] T. Ozawa, Kinetic of non-isothermal crystallization, Polymer 12 (1971) 150–158.

[18] C.T. Cheng, M. Lanagan, B. Jones, J.T. Lin, M.J. Pan, Crystallization kinetic and phase development of PbO-BaO-SrO-Nb_2O_5-B_2O_3-SiO_2-based glass-ceramics, J. Am. Ceram. Soc. 88 (2005) 3037–3042.

[19] A.A. Francis, Non-isothermal crystallization kinetics of a blast furnace slag glass, J. Am. Ceram. Soc. 88 (2005) 1859–1863.

[20] K. Matusita, S. Sakka, Kinetics study of crystallization of glasses by differential scanning calorimeter, Phys. Chem. Glasses 20 (1979) 81–84.

[21] K. Matusita, S. Sakka, Kinetics study on crystallization of glass by differential thermal analysis-criterion on application of Kissinger plot, J. Non-Cryst. Solids 38–39 (1980) 741–746.